Fedorenko, A., Kryuchkov, E., & Voitsekhovska, A. (2025).
Wind as an energy source of polar atmospheric gravity waves.
Ukrainian Antarctic Journal, *23*(1), 19–31.
https://doi.org/10.33275/1727-7485.1.2025.741

Wind as an energy source of polar atmospheric gravity waves

Alla Fedorenko*, Evgen Kryuchkov, Anna Voitsekhovska
Space Research Institute of the National Academy of Sciences of Ukraine and State Space Agency of Ukraine, Kyiv, 03187, Ukraine
*** Corresponding author:** fedorenkoak@gmail.com

Abstract. We investigated the properties of atmospheric gravity waves (AGW) in the areas of polar thermosphere wind systems using satellite measurement data. It was established that AGWs systematically propagate in the direction from night to day towards the wind. The dependence of the wave amplitude on the headwind wind velocity was studied. In an oncoming non-uniform wind flow, wave amplitudes increase due to energy exchange with the medium. As a result, such large-amplitude AGWs are predominant in observations in the polar thermosphere. Therefore, wind flow regions can be considered a source of energy for AGW. The frequencies of polar AGW were determined from satellite measurements. The obtained frequency values for different polar orbits of the Dynamics Explorer 2 satellite are very close to the Brunt-Väisälä (BV) frequency. This indicates the filtering of the wave spectrum in the non-uniform wind flow. The results allow us to explain the main properties of AGW in the polar thermosphere observed from the satellite and compare them with ground-based measurements. When comparing the results of satellite and ground measurements of AGW characteristics, background atmospheric flows must be taken into account. Thus, the frequencies of AGW determined from satellite data are close to the Brunt-Väisälä frequency. However, a ground observer will register such waves as very low-frequency disturbances. It can be assumed that some of the observed cases of large-scale AGW are medium-scale disturbances propagating against the background of strong winds. Under increased geomagnetic activity, the speeds of polar vortices increase, accompanied by an increase in energy transfer from the wind. Therefore, AGWs play an important role in the energy balance of the polar atmosphere, redistributing the energy of disturbed wind flows in the vertical direction.

Keywords: non-uniform wind flow, polar thermosphere, waves in the atmosphere, wind filtering

1 Introduction

Atmospheric gravity waves (AGW) play an important role in the redistribution of disturbance energy on a planetary scale (Liu et al., 2024). They also provide energy coupling between different high-altitude levels of the atmosphere (Hines, 1960; Nappo, 2012). During the propagation of AGW from localized sources, the waves interact with the atmospheric environment. This has a significant impact on the energy balance of the atmosphere.

Two factors determine AGWs' energy. One is the energy of sources: more powerful sources generate AGWs of large amplitudes, which carry, accordingly, a significant flow of wave energy in space. Secondly, these waves propagate in the atmosphere, leading to losses through dissipation and amplification under certain conditions. Thus,

AGWs' features can be determined to a greater extent by the properties of the environment than by the properties of the sources. Effective energy exchange between AGW and the medium occurs in spatially heterogeneous wind flows (Lighthill, 1978; Fedorenko et al., 2018). The neutral atmospheric medium is a giant reservoir of energy, compared to the energy of the AGW. Therefore, if there is some energy transfer channel from the medium, the energy and the waves' amplitudes can increase significantly.

In the classical AGW theory, without taking into account the exchange of energy with the environment, the wave amplitude increases with height due to the exponential decrease in the density of the atmosphere, but the energy density is conserved (Hines, 1960; Nappo, 2012). In the presence of spatially heterogeneous wind, energy can be exchanged between the environment and the AGW. Fedorenko et al. (2024) recently studied changes in the amplitudes of AGWs propagating in a horizontally heterogeneous flow. It is shown that for AGWs moving against the wind, energy flows from the environment to the waves. On the contrary, waves traveling with the wind release energy and quickly decay. Harvey et al. (2023) report experimental evidence of the connection between the AGW and the Arctic and Antarctic polar vortices at mesospheric altitudes.

The polar thermosphere is a unique area for studying such energy transfers. The most powerful sources of disturbances in the upper atmosphere associated with geomagnetic activity are over the Arctic and Antarctic. These sources generate atmospheric waves of various types, including AGW (Rourke et al., 2017; Moffat-Griffin, 2019). In the polar regions, powerful spatially heterogeneous wind systems are formed. The specifics of polar thermosphere circulation have been actively studied theoretically and experimentally (Thayer et al., 1987; Aruliah et al., 1991; Deng & Ridley, 2006; Lühr et al., 2007). The main feature of the wind circulation in the polar thermosphere is vortices with horizontal dimensions of ~ several thousand km. Polar vortices arise in the morning and evening sectors near the polar region due to the involvement of the neutral medium in the movement of ionospheric plasma, which drifts in the crossed fields of magnetospheric-ionospheric convection. In between the vortices, there is a spatially heterogeneous flow directed mainly from the Sun. The speed of this flow, depending on solar and geomagnetic activity, is ~300–700 $m \cdot s^{-1}$ (Killeen et al., 1995; Lühr et al., 2007). This flow is superimposed on a gradient wind caused by the absorption of solar ultraviolet radiation, the speed of which at the thermospheric heights usually does not exceed 250 $m \cdot s^{-1}$. As the Earth rotates, polar vortex's geographical coordinates change; the superposition of the gradient wind with the eddy flow is complex.

As a result, the horizontal structure of flows in the polar thermosphere is quite uneven. The polar wind configuration is determined to a greater extent by magnetosphere-ionosphere interaction than by insolation conditions. The higher the geomagnetic activity, the greater the contribution of the eddy component to the wind configuration and the greater the wind speed. Thus, the simulation showed that the wind speed in the polar cap at an altitude of 250 km correlates with the magnitude of the southern Bz component of the Interplanetary Magnetic Field (Deng & Ridley, 2006). When AGWs propagate in the polar thermosphere with complex dynamics, it can be expected that the observed characteristics of the waves will be only partially determined by the sources, and the properties of the environment will play a significant role. This greatly complicates a ground-based experimental diagnosis of waves and the search for a connection with their sources.

The propagation of AGW at ionospheric heights is manifested by the corresponding disturbances in the ionosphere, which can be registered by ground-based remote methods. For some time, the theory of AGW in a neutral atmosphere was developed in isolation from observations of travelling ionospheric disturbances (TIDs). Hines (1960) first suggested that most of the observed TIDs are manifestations of the propagation of AGW in the neu-

tral atmosphere. Ground-based observations of travelling ionospheric disturbances in the polar regions show periods corresponding to the freely propagating AGWs. In particular, the characteristic periods of AGW (tens of minutes) are often visible in auroral events (electrojet variations, particle discharges, etc.) considered hypothetical sources of polar wave disturbances (Crowley & Williams, 1987; Williams et al., 1992).

TIDs over the Antarctic Peninsula were described quantitatively using the Global Navigation Satellite System Total Electron Content and High Frequency sounding observations (Paznukhov et al., 2022). Periods of TIDs significantly differ between the seasons. Wintertime TIDs have noticeably shorter periods (10–50 min) compared to the rest of the year (30–140 min). The seasonal variation of TIDs over Alaska is examined using the Poker Flat Radar (Negale et al., 2018). In contrast, satellite data indicate a predominance of AGW with frequencies close to Brunt-Väisälä (BV) frequency in both polar thermospheres (Innis & Conde, 2002; Fedorenko et al., 2015). Such a significant difference between the properties of AGWs observed from satellite and ground-based measurements requires an explanation. In our opinion, these differences are due to the propagation of waves in powerful wind flows.

Extremely high speeds of wind flows and their spatial heterogeneity shape the propagation of AGW in the polar regions. The area between the polar thermospheric vortices can be considered as a source of energy for AGW. The properties of this wind source were studied. The experimental results, which were mainly obtained in our previous studies, will be briefly analysed. Theoretical mechanisms of selective amplification of the amplitudes of AGWs with certain spectral properties are considered. Significant differences between satellite and ground-based observations of AGW propagating in powerful atmospheric flows are analyzed. An alternative interpretation of the observed large-scale TIDs is proposed as a consequence of the propagation of medium-scale waves in the wind flow.

2 Data and methods

Our research is based on atmosphere parameters measured using the low-orbit polar satellite Dynamics Explorer 2 (DE2). The orbital configuration of the DE2 satellite (altitude of 250–1000 km, orbital plane inclination of 89.9°) is very convenient for studying the polar regions in both hemispheres. Conditions for studying wave activity over the Antarctic are more favorable since the orbital perigee was in the southern polar regions for most of the DE2 mission. The satellite's complex of scientific equipment included sensors of the parameters of the neutral and plasma components of the atmosphere (Carignan et al., 1981; Spencer et al., 1981). These data make it possible to study the AGW based on *in situ* measurements of variations in the velocity, temperature, and concentration of neutral particles.

To study the relationship between AGW and wind, we used measurement data obtained in three experiments on board the DE2 satellite: NACS (Neutral Atmosphere Composition Spectrometer) (Carignan et al., 1981), WATS (Wind and Temperature Spectrometer) (Spencer et al., 1981) and FPI (Fabry-Perot interferometer) (Hays et al., 1981). In the NACS experiment, the concentrations of neutral atmospheric components, such as atomic oxygen O, molecular nitrogen N_2, argon Ar, and other atmospheric gases, were measured using a mass spectrometer. The temperature and vertical velocity of neutral particles were measured in the WATS experiment. The horizontal component of the velocity of neutral particles along the satellite orbit was measured in the FPI experiment using a Fabry-Perot interferometer based on the Doppler shift frequency of the red oxygen line O 630.0 nm.

We used the data from the NACS experiment to determine the amplitudes of the AGW in atmospheric density fluctuations, as well as the directions of wave propagation. The 1-s averaged concentration measurement data were obtained from the https://spdf.gsfc.nasa.gov/pub/data/de/de2/neutral_gas_nacs database. The hypothetical

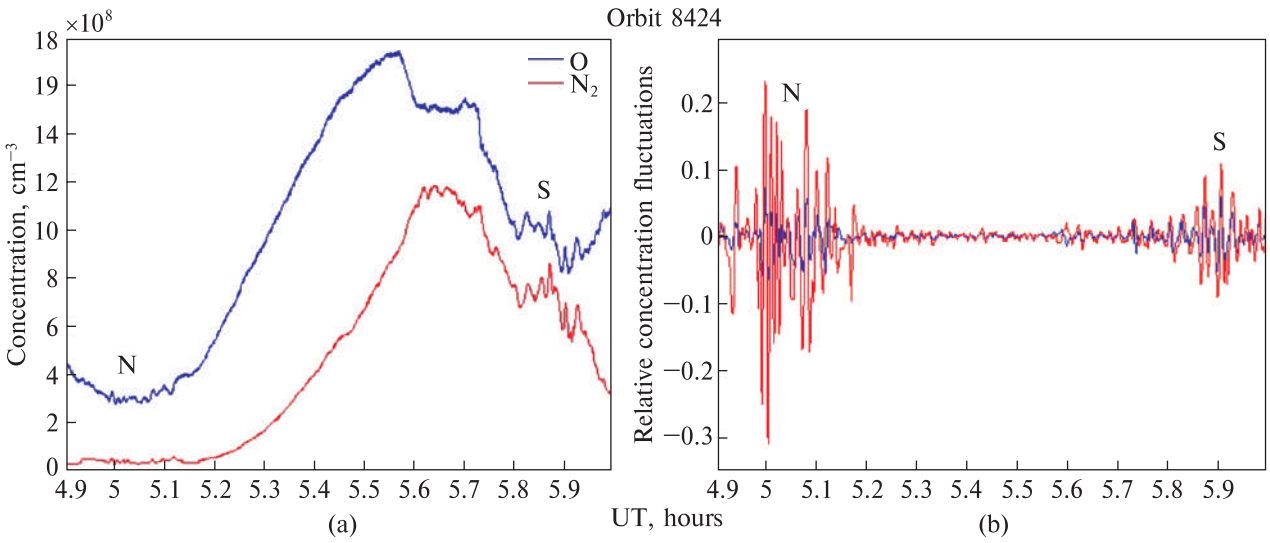

Figure 1. (a) Concentrations of n(O) and n(N_2) and (b) fluctuations of δn(O)/n(O) and δn(N_2)/n(N_2) on orbit 8424 of the Dynamics Explorer 2 satellite

possibility of determining the directions of wave propagation from measurements of the concentrations of individual gases is due to the fact that above the turbopause, all atmospheric gases are distributed with height according to their individual height scales. Due to this, in the satellite observations of the AGW in the thermosphere, we clearly see how the lighter gas is ahead of the heavier gas in the direction of wave propagation (Fedorenko, 2009). This allows us to determine the directions of the AGW at the heights of the thermosphere from fluctuations in the concentrations of various gases.

The measured values of the concentrations n(O) and n(N_2) on the 8424 orbit are shown in Figure 1a. The orbital height varied from ~320 km above the northern polar region to ~250 km above the southern polar region. In the higher part of the orbit, n(O) is an order of magnitude higher than n(N_2); in the lower part, these values converge. Over both polar regions, wave-like fluctuations in both gases under consideration are noticeable. To separate these wave fluctuations from large-scale concentration changes, a moving average window was used. After applying the moving average procedure, we find the fluctuations δn(O) and δn(N_2) as the difference between the original and averaged data. The window sizes were chosen based on the criterion of maximum correlation of the obtained fluctuations δn(O) and δn(N_2). The basis of this approach is the obvious assumption that the same wave process is observed in both types of gases.

Relative fluctuations δn(N_2)/n(N_2) and δn(O)/n(O) are usually considered in the theory of AGW. This makes it possible to eliminate significant differences in the absolute values of the concentrations of these gases in the atmosphere. The values of δn(N_2)/n(N_2) and δn(O)/n(O) obtained from satellite measurements on orbit 8424 (February 1, 1983) are shown in Figure 1b. A significant increase in the amplitudes of concentration fluctuations over both polar regions compared to mid-latitudes is visible. In more detail, the nature of the fluctuations δn(N_2)/n(N_2) and δn(O)/n(O) directly over the polar regions is shown in Figure 2a, b. The magnitude of relative fluctuations in the heavier gas N_2 reaches 10–20%; in atomic oxygen O, it does not exceed 5%. This ratio of amplitudes in different atmospheric gases is consistent with theoretical ideas about the propagation of AGW in the thermosphere (Fedorenko et al., 2015). It is also clearly seen that over the northern polar re-

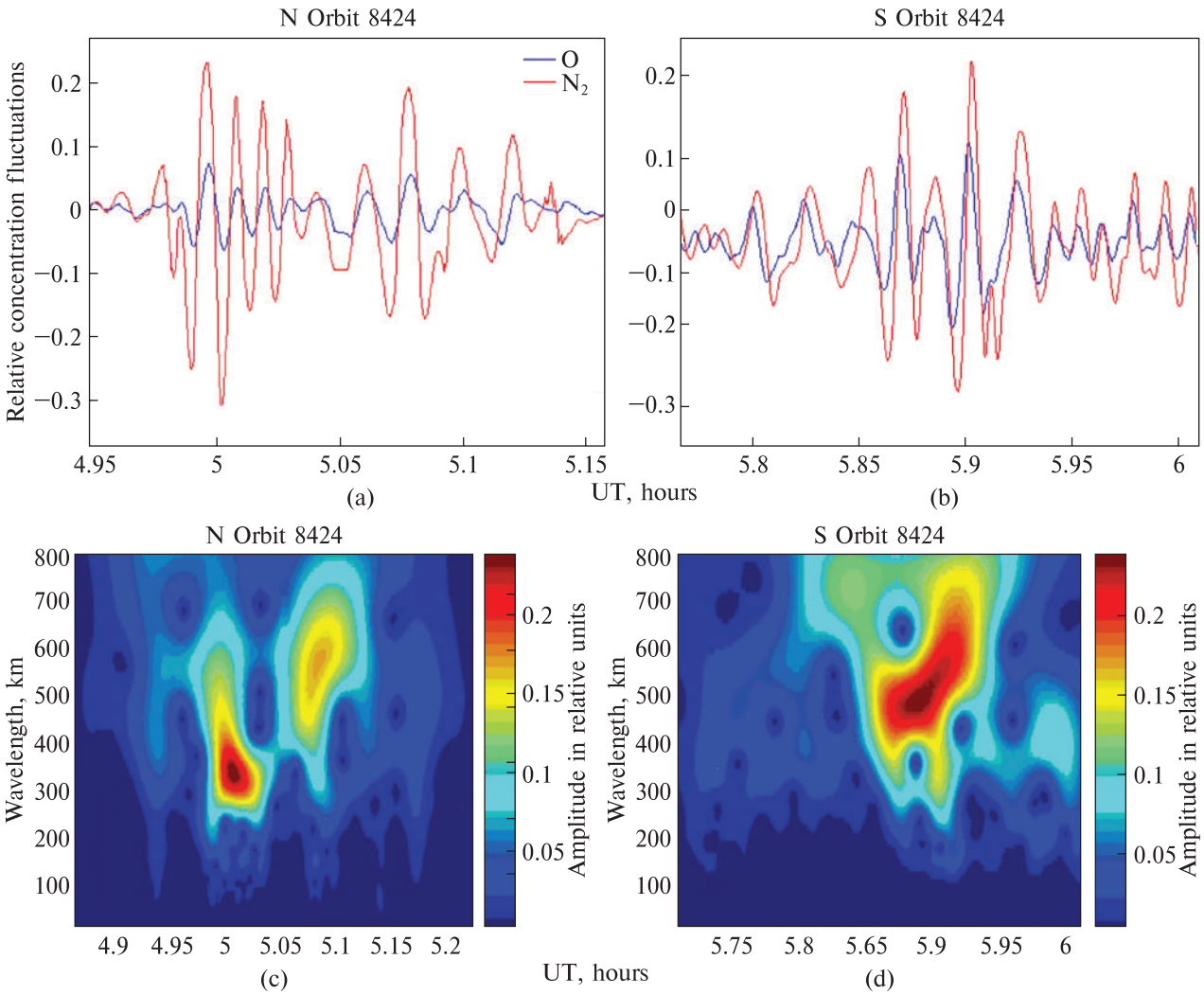

Figure 2. Fluctuations of $\delta n(O)/n(O)$ and $\delta n(N_2)/n(N_2)$ on the 8424 orbit in the northern (a) and southern (b) polar regions and amplitude wavelet spectra for $\delta n(N_2)/n(N_2)$ (c, d)

gion, fluctuations $\delta n(O)/n(O)$ are ahead of $\delta n(N_2)/n(N_2)$ fluctuations in phase. Over the southern polar region, on the contrary, fluctuations $\delta n(O)/n(O)$ lag behind $\delta n(N_2)/n(N_2)$. A simple way to determine the direction of AGW propagation along the satellite's orbit is based on the analysis of these phase shifts (Fedorenko, 2009).

When studying wave processes from aboard a satellite, there is always a problem of separating spatial and temporal changes in the measured parameters. Thus, the frequency Ω, which is measured from aboard a moving satellite, is shifted due to the Doppler effect $\Omega = \Omega_0 - k_{xs} \cdot V_s$. Here Ω_0 is the frequency in a fixed reference frame, k_{xs} is the component of the wave vector along the orbit, $V_s \approx 8$ km $\cdot$ s^{-1} is the speed of a low-orbit satellite. The phase horizontal velocities of AGW are usually several hundred m $\cdot$ s^{-1} (Hines, 1960). Therefore, the spectrum of wave numbers $\Omega \approx k_{xs} \cdot V_s$ is actually measured onboard the satellite. That is, the propagation of AGW is recorded in the form of quasi-stationary periodic structures in the distribution of atmospheric parameters, such as concentration, temperature, and velocity. The hori-

zontal scales of polar AGW observed on the DE2 satellite were mainly λ_{xs} = (45–70)s · 8 km · s^{-1} = = 360–560 km. Here, the quantity λ_{xs} denotes the projection of the horizontal wavelength onto the satellite's orbit. The true horizontal wavelengths λ_x differ from λ_{xs} depending on the angle at which the satellite crosses the wavefront.

Due to the impossibility of directly measuring the AGW frequency from the satellite, we determined it based on measurements of atmospheric parameters in the WATS and NACS experiments. In this case, the well-known relationship $V_z = i\omega h$ was used (Innis & Conde, 2002). Here, V_z is the vertical velocity of particles, h is the vertical displacement of the elementary volume of the medium during the AGW propagation. The value of the vertical component of the velocity V_z was directly measured in the WATS experiment. The value of h can be approximately calculated from measurements of the concentrations of two gases (Fedorenko, 2009): $h = F \cdot [\delta n(N_2)/n(N_2) - \delta n(O)/n(O)]$. Here, $F = H(O)H(N_2)/[H(O)-H(N_2)]$; H(O) and $H(N_2)$ are individual scale heights of gas concentrations in the thermosphere.

To study the relationship between the AGW amplitudes and the wind velocity, data from the FPI experiment were used. The values (along the orbit) component of the wind velocity, averaged over 16 s, are presented in the database https://spdf.gsfc.nasa.gov/pub/data/de/de2/neutral_gas_fpi/.

Table. Directions of AGW propagation in polar regions

Hemisphere	Month	Orbit number	Height, km	$\delta\rho \cdot \rho^{-1}$, %	Latitude, degrees	LT, hours	Sign of $\Delta\varphi$	Direction
1	2	3	4	5	6	7	8	9
S	July	5424	370−300	4.5	63−72	2.0−14.0	+	→
S	July	5454	370−300	5	56−80	1.8−13.8	+	→
S	July	5462	420−320	4	63−74	1.8−13.8	+	→
S	July	5487	350−310	3.5	56−76	1.7−13.7	+	→
S	July	5500	340−310	5	55−72	1.6−13.6	+	→
N	July	4983	300−400	2	67−68	15.9−3.9	-	←
N	July	4984	300−430	3	70−59	15.9−3.9	-	←
N	July	4986	310−430	4	74−57	15.9−3.9	-	←
N	July	4991	290−370	3	70−67	15.9−3.9	-	←
N	July	5053	300−400	5	67−62	15.6−3.6	-	←
S	January	8216	270−250	5.5	67−35	13.9−1.9	-	←
S	January	8257	280−250	5	66−45	13.8−1.8	-	←
S	January	8273	265−250	4	73−50	13.7−1.7	-	←
S	January	8286	260−250	2.5	70−32	13.6−1.6	-	←
S	January	8303	260−250	5	70−55	13.6−1.6	-	←
N	January	8192	340−370	13	62−78	2.0−14.0	+	→
N	January	8196	340−375	7.5	59−72	2.0−14.0	+	→
N	January	8201	340−370	4	75−81	2.0−14.0	+	→
N	January	8205	340−370	5	68−77	2.0−14.0	+	→
N	January	8206	340−375	6	59−77	2.0−14.0	+	→

Here, 1 − hemisphere; 2 − month of the year; 3 − orbit number; 4 − change in orbital height within the wave train; 5 − average amplitudes within the wave train $\delta\rho \cdot \rho^{-1}$, %; 6 − geographical latitude within the wave train; 7 − solar local time (LT); 8 − sign of phase shift $\Delta\varphi$ between fluctuations $\delta n(O)/n(O)$ and $\delta n(N_2)/n(N_2)$ along the orbit; 9 − direction of AGW propagation ("→" − in the same direction as the satellite, "←" − towards the satellite)

The wind speed in the FPI experiment was determined by the limb scanning method using the Doppler shift frequency of the atmospheric emission O 630.0 nm (Hays et al., 1981). Since the inclination of the DE2 satellite orbit was 89.9°, the meridional component of the wind speed was actually measured in the FPI experiment.

3 Results

3.1 AGW propagation directions

The DE2 orbit with an inclination of 89.9° was polar sun-synchronous. When a satellite passes near the poles, the solar local time LT changes to LT ± ± 12^h. For most of the duration of the DE2 mission, the orbit was synchronized in such a way that a day-night or night-day transition occurred near the poles. During these sharp changes in local time, systematic patterns in the phase shifts between the fluctuations $\delta n(O)/n(O)$ and $\delta n(N_2)/n(N_2)$ were observed. These features are shown in Table using the example of 20 orbits of the DE2 satellite for polar day and polar night conditions in both hemispheres (5 orbits for different conditions). As seen from the Table, in the range of time zones 1.6–3.9^h LT (13.6–15.9^h LT), a systematic direction of AGW propagation from night to day is observed. It looks as if there is a regular source of waves in the night sector of the polar region.

On the other hand, it is known that the wind blows mainly from the Sun. Therefore, we conclude that the waves propagate against the wind. This suggested a closer interaction of polar AGWs with the wind and was an impetus for further experimental and theoretical studies. The azimuths of AGW propagation for the northern polar region under the polar day and night conditions are shown in Figure 6 in (Fedorenko et al., 2015).

3.2 Dependence of wave amplitude on wind speed

According to the data of synchronous measurements of density in the NACS experiment and wind speed in the FPI experiment, the dependence of the amplitudes of polar AGWs on the background wind

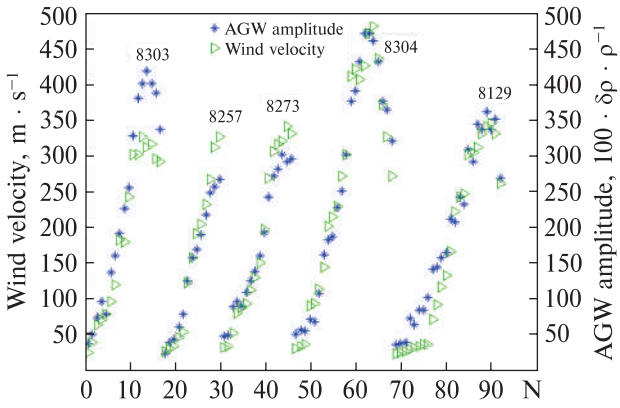

Figure 3. AGW amplitude ($100 \cdot \delta\rho \cdot \rho^{-1}$) and meridional wind velocity ($m \cdot s^{-1}$) along 5 sections of the orbits of the DE2 satellite over the southern polar region. N are the counts along the orbits when wind speed measurements were made

was investigated. Figure 3 simultaneously shows the values of wind speed and AGW amplitudes along several sections of the satellite orbits in the southern polar region. The average values of AGW amplitude in the wave train are considered here. For clarity, the AGW amplitude is shown in units of $100 \cdot \delta\rho \cdot \rho^{-1}$ (%). As shown in Figure 3, the relationship between AGW amplitudes and wind speed along individual orbits is clearly visible.

A theoretical analysis of the change in AGW amplitude in the non-uniform wind flow was recently done by Fedorenko et al. (2024). In this work, a system of modified hydrodynamic equations was obtained, taking into account the components that describe the linear interaction of waves with a non-uniform flow. Based on the analysis of this system, with slow changes in wind speed on wavelength scale, the spatial heterogeneity of the wind actually does not affect the dispersion equation but only the wave amplitudes. The dependence of the AGW amplitude on the wind speed is described by the following approximate equation (Fedorenko et al., 2024):

$$A \approx A_0 (W_x / W_{x0}) \exp\left[- x \frac{\partial W_x}{\partial x} \left(\frac{1}{U_x} + \frac{\gamma}{4 c_s^2} (U_x + W_x) \right) \right]$$

Here, W_x is the wind velocity, $U_x = \omega / k_x$ is the phase horizontal velocity of the AGW, γ is the

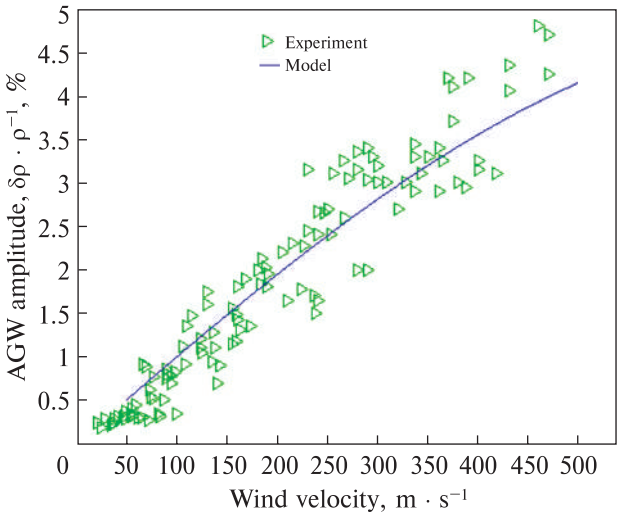

Figure 4. Experimental and model dependencies of AGW amplitude on wind velocity

ratio of specific heats, and $c_s = (\gamma gH)^{(1/2)}$ is the speed of sound. According to this equation, the dependence of the AGW amplitude on the wind speed consists of a linear and an exponential part. The linear part is related to changes in the background parameters of the medium and does not depend on the direction of wave propagation relative to the flow. The exponential part is caused by inertial forces (Fedorenko et al., 2024). It gives an increase in the amplitude of the waves in the headwind flow ($\delta W_x/\delta x < 0$) and its rapid attenuation in the accompanying wind ($\delta W_x/\delta x > 0$). The linear dependence of the amplitude on the wind speed prevails in the case of a headwind, and the exponential part only slightly slows down the growth of the wave amplitude at high values of the wind speed $W_x > 350$ m · s^{-1}. However, the exponential part provides a very rapid decrease in the amplitude with increasing tailwind speed.

Figure 4 shows the change in AGW amplitude in the headwind according to experimental data and modeling results based on the data of Fedorenko et al. (2024). For calculations, a heterogeneous wind is taken, the speed of which increases linearly from 50 m · s^{-1} to 500 m · s^{-1} with a spatial gradient ($\delta W_x/\delta x$) ≈10^{-5} s^{-1}. This satisfies the condition of slow changes in wind speed for the typical scales of AGW in the upper atmosphere from hundreds to several thousand km. Theoretical dependencies agree well with the experimental data, except for very small and large wind speeds. The change in the AGW amplitude directly shows how the wave energy increases due to the interaction with the medium. The relative change in wave energy is proportional to the square of the change in amplitude $E/E_0 \sim (A/A_0)^2$.

3.3 Polar AGW frequencies

Fluctuations in the magnitude V_z lead to fluctuations of h in phase by $\pi/2$ in the direction of AGW propagation according to measurements on the DE2 satellite (Fedorenko et al., 2015). We used the ratio of the amplitudes of these quantities to determine the wave frequency. The experimental dependence of $V_z(h)$ is shown in Figure 5 according to measurements on polar parts of several DE2 satellite orbits. The AGW frequency determined using linear approximation is, on average, 0.01 s^{-1}. Note that the frequencies of polar AGW determined from satellite data are frequencies in the reference frame of the medium. This value corresponds to the period $T = 2\pi/\omega = 628$ s. At the same time, the Brunt-Väisälä period for the conditions of satellite observations is ~10 min. That is, the determined value of the period of polar AGW is very close to the period of BV. Background horizontal temperature trends affect the values of the quantities H(O) and H(N_2), which are used in calculating the vertical displacement h (Fedorenko, 2009). Therefore, the value of the frequency determined from satellite data is approximate.

It is also necessary to another limitation of the above-mentioned frequency determination method. We assumed a monochromatic plane wave $V_z = i\omega h$, while the wave trains are not monochromatic, at least in the measured wavelengths. Scattering of the measured values of λ_{xs} can be partly caused by different projections of wave vectors onto the satellite's orbit. However, as seen in Figure 2, the values of λ_{xs} are not monochromatic even within the same wave train. In this regard,

it is important that the considered method of determining the frequency of the AGW is not based on the measured projection of the wavelength but only on the ratio of the amplitudes of the quantities V_z and h. Even under such limitations, it is clear that the frequencies of polar AGWs are high and close to the value of BV frequency. Various energy processes occur in the auroral oval, which lead to the generation of a wide spectrum of waves. Therefore, a hypothetical source is unlikely to systematically generate the same type of AGW with such high frequencies. It is more reasonable to assume that the predominance of high frequencies results from the interaction of waves with the medium.

Fedorenko et al. (2018) theoretically investigated the possibility of filtering the spectrum of primary AGWs that enter a spatially heterogeneous wind flow. The results were obtained under the assumption of weak spatial inhomogeneity of the flow when the AGW dispersion equation is locally satisfied at each point of the moving medium (Lighthill, 1978). In such an assumption, it is possible to switch to the reference frame of the moving medium. For the frequency $\omega = \omega_0 - k_x \cdot W_x$ in the reference frame of the medium, the form of the differential hydrodynamic equations remains the same as for a stationary medium. Here, ω_0 is the frequency in the stationary reference frame, and k_x is the horizontal component of the wave vector. Accordingly, the dispersion equation obtained also retains its form. After substituting the AGW dispersion equation for the headwind frequency $\omega = \omega_0 + k_x \cdot W_x$, we obtain a family of dispersion curves (see Fig. 1 in (Fedorenko et al., 2018)). These dispersion curves are modified depending on the wind speed. The curves have a maximum $\delta\omega_0/\delta k_x = U_{gx0} = 0$, where U_{gx0} is the group velocity in a stationary frame of reference. The group velocity of a wave for a stationary observer in a headwind is $U_{gx0} = U_{gx} - W_x$, where U_{gx} is the group velocity in the reference frame of the medium. The condition $\delta\omega/\delta k_x = U_{gx} = W_x$ is satisfied at the points of maxima. When U_{gx} in the medium is equal in magnitude to the wind speed $U_{gx0} = 0$, the wave is blocked in the headwind.

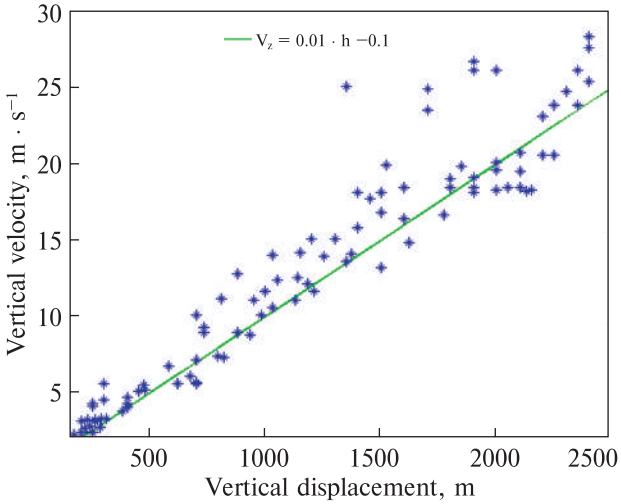

Figure 5. Dependence of vertical velocity on vertical displacement in polar AGWs

Fedorenko et al. (2018) showed that the horizontal scale of the blocked waves tends to some limiting value $k_x \to 4\pi H$. This scale corresponds to the horizontal wavelength $\lambda_x = 350-550$ km, depending on the value of H, which is most often recorded in satellite observations of polar AGWs (Innis & Conde, 2002; Fedorenko et al., 2015).

Therefore, the high frequencies of polar AGWs are probably a consequence of filtering these waves in the wind flow. Let us assume that AGWs with a frequency of ω_0 during propagation enter the non-uniform wind. Then, in a headwind, the AGW frequency in the medium reference frame $\omega = \omega_0 + k_x \cdot W_x$ increases rapidly with increasing wind speed, reaching the limiting values up to the frequency of the BV. Therefore, the systematic predominance of high frequencies in the spectrum of polar AGWs indicates the filtering of primary waves, which could have had different initial frequencies ω_0.

4 Discussion

Wave activity in the polar regions is studied mainly by observations of TIDs (Zhang et al., 2019; Paznukhov et al., 2022). This is due to the large amount of available experimental data and nu-

merous methods for determining the state of the ionosphere. Experimental studies of AGW in the neutral atmosphere based on direct measurements from satellites are significantly limited (Johnson et al., 1995; Innis & Conde, 2002; Fedorenko et al., 2015) as there are not enough low-orbit satellites equipped for such measurements.

According to long-term observations, travelling ionospheric disturbances are divided into large-scale and medium-scale TIDs (Francis, 1975; Hocke & Schlegel, 1996). Medium-scale TIDs have horizontal phase velocities of 100–250 m · s^{-1}, periods of 15 min – 1 h, and horizontal wavelengths of ~ several hundred km. It is believed that such TIDs/AGWs can be generated by sources at any altitude level in the atmosphere, including in the troposphere or on the Earth's surface. Medium-scale AGWs are considered important agents connecting the lower and upper atmosphere. They do not show a pronounced correlation with geomagnetic activity.

Large-scale TIDs propagate with horizontal phase velocities of 400–1000 m · s^{-1}; their periods are from ~30 min up to ~3 h, and horizontal wavelengths exceed 1000 km. Such TIDs mainly propagate from the polar regions. The frequency of their appearance correlates with geomagnetic storms and variations of the auroral electrojet (Hajkowicz, 1991). Tsugawa et al. (2004) determined the following characteristics of large-scale TIDs over Japan based on measurements of the GPS network: phase horizontal velocities of 475 ± 171 m · s^{-1}, periods of 80 ± 29 min, wavelengths of 2131 ± ± 863 km. According to these studies, the frequency of large-scale disturbances increases significantly with the increase of the K_p index. Differences between the spectral properties of large- and medium-scale AGWs/TIDs are usually explained by different generation mechanisms (Francis, 1975). Large-scale TIDs are considered to be waveguide modes generated by auroral sources at the heights of the E-region of the ionosphere (Francis, 1975). Medium-scale TIDs are manifestations of freely propagating AGWs that can occur at different altitude levels of the atmosphere.

Direct satellite measurements differ significantly from ground-based observations of AGWs/TIDs in terms of obtaining information on their spectral properties. A ground-based observer measures the AGW period and can also determine the phase horizontal velocity using multi-station measurements. The wavelength along the orbit is measured from the satellite *in situ*. Synchronising measurements of various parameters (such as velocity and concentration of particles) makes it possible to determine the period in the reference frame of the medium (Fedorenko et al., 2015). Satellite observations show that in the polar regions, AGWs systematically propagate against the background of powerful wind systems and, as a result, closely interact with them. Thus, information on the spectral properties of wave disturbances obtained from ground observations can be significantly distorted by winds. In the polar thermosphere, where wind speeds often exceed the characteristic horizontal phase velocities of AGWs, these effects are most noticeable.

The peculiarities of the interaction of AGWs with wind flows allow us to consider an alternative explanation of the difference in the characteristics of large- and medium-scale AGWs/TIDs. It can be assumed that many ground-observed large-scale TIDs may be medium-scale waves "disguised" by powerful wind flows. According to satellite measurements, polar AGWs systematically move against the wind. Therefore, such disturbances are registered by the ground observer with frequencies $\omega_0 = \omega - k_x W_x$ reduced due to the Doppler effect and, accordingly, with longer periods. According to the satellite data, polar regions are dominated by AGWs with horizontal wavelengths of 450–600 km, with frequencies close to the Brunt-Väisälä frequency (Innis & Conde, 2002; Fedorenko et al., 2015). These parameters are characteristic of AGWs near the blocking point on the opposite flow, which are significantly amplified in amplitude (Fedorenko et al., 2018). At typical wind speeds of 300–600 m · s^{-1}, the periods of these AGWs measured by a ground observer will be from 30 min up to 1 h. Wind speed

in the polar thermosphere is actually never less than 250 m · s^{-1}, so the minimum observed TID periods are about 20 minutes. With high geomagnetic activity, the disturbed wind in the thermosphere can reach ~700 m · s^{-1}. Against the background of such a strong wind, wave periods for a ground observer can exceed 2 h, corresponding to large-scale AGW/TID periods.

In the proposed interpretation, the large-scale AGWs/TIDs observed in the polar regions acquire their properties as a result of interaction with the wind. The wind flow filters the spectrum, sets the prevailing azimuths of propagation, and amplifies the AGW amplitudes. With the growth of geomagnetic activity and the increase of wind speed in the thermosphere, the frequency of occurrence of TIDs with long periods is expected to increase. Under this consideration, the properties of large-scale TIDs are determined not by the power of their generation sources, with which it is quite difficult to establish a direct relationship, but by the disturbed inhomogeneous flow in the polar thermosphere.

5 Conclusions

We have investigated the manifestations of the interaction of AGW with wind in the region of polar wind systems using satellite measurements. According to experimental data, it was established that AGWs in the polar thermosphere systematically propagate from night to day against the wind. The dependence of the amplitude of these waves on the wind speed was studied. The increase in the AGW amplitudes due to energy transfer from the medium is observed in a spatially inhomogeneous headwind. This provides amplification of AGW to significant amplitudes, making them clearly visible and predominant in observations. It should be noted that the key factor for such energy exchange is precisely the spatial inhomogeneity of the wind flow. When AGW propagates in a homogeneous flow, a Doppler frequency shift is observed for a stationary observer, and no changes in wave amplitudes occur. The frequencies of polar AGWs have been determined from satellite measurements. The obtained frequency values are very close to the BV frequency. In our opinion, this indicates filtering of the AGW spectrum in the wind flow. The results allow us to explain the main properties of AGW in the polar thermosphere observed from the satellite.

The non-uniform wind can be considered the main source of AGW in the polar thermosphere in the sense that the wind determines the prevailing directions of propagation, frequencies, and amplitudes of these waves. There is always a background wave field in the thermosphere due to the superposition of small-amplitude AGWs originating from different sources. It does not matter how the primary waves arose. These waves may have different initial spectral characteristics. However, when AGWs enter the region of the polar non-uniform wind flow, filtering and selective amplification of the amplitudes of certain spectral harmonics occur. As a result, large-amplitude AGWs that move upwind and have frequency ~ the BV frequency are predominantly observed in polar regions.

In order to compare these results with the characteristics of the TIDs obtained in ground measurements, it is necessary to consider the background atmospheric flows. We offer an alternative explanation of the observed large-scale AGW/TID that occurs in the polar regions mainly during geomagnetic storms. It is assumed that some of the cases of large-scale AGWs are medium-scale disturbances that change due to propagation against the background of strong inhomogeneous winds. Waves moving against strong winds will be registered by a ground observer as long-period TIDs, with their amplitudes significantly enhanced by interaction with the wind.

Author contributions. Investigation and interpretation, E. K. and A. V.; writing and preparation of the article, A. F.; editing, A. V.

Funding. This work was supported by the State Institution National Antarctic Scientific Center of the Ministry of Education and Science of Ukraine within the framework of the State Special-

Purpose Research Program in Antarctica for 2011–2025.

Conflict of Interest. The authors declare no conflict of interest.

References

Aruliah, A. L., Rees, D., & Fuller-Rowell, T. J. (1991). The combined effect of solar and geomagnetic activity on high-latitude thermospheric neutral winds. Part I. Observations. *Journal of Atmospheric and Terrestrial Physics*, *53*(6–7), 467–483. https://doi.org/10.1016/0021-9169(91)90075-I

Carignan, G. R., Block, B. P., Maurer, J. C., Hedin, A. E., Reber, C. A., & Spencer, N. W. (1981). The neutral mass spectrometer on Dynamics Explorer B. *Space Science Instrumentation*, *5*, 429–441. https://ntrs.nasa.gov/citations/19820032902

Crowley, G., & Williams, P. J. S. (1987). Observation of the source and propagation of atmospheric gravity waves. *Nature*, *328*, 231–233. https://doi.org/10.1038/328231a0

Deng, Y., & Ridley, A. J. (2006). Dependence of neutral winds on convection E-field, solar EUV, and auroral particle precipitation at high latitudes. *Journal of Geophysical Research. Space Physics*, *111*(A9), A09306. https://doi.org/10.1029/2005JA011368

Fedorenko, A. K. (2009). Determination characteristics of atmospheric gravity waves in the Polar regions using mass-spectrometer satellite measurements. *Radio Physics and Radio Astronomy*, *14*(3), 254–266. http://rpra-journal.org.ua/index.php/ra/article/view/510 (In Ukrainian)

Fedorenko, A. K., Bespalova, A. V., Cheremnykh, O. K., & Kryuchkov, E. I. (2015). A dominant acoustic-gravity mode in the polar thermosphere. *Annales Geophysicae*, *33*(1), 101–108. https://doi.org/10.5194/angeo-33-101-2015

Fedorenko, A. K., Kryuchkov, E. I., Cheremnykh, O. K., Klymenko, Yu. O., & Yampolski, Yu. M. (2018). Peculiarities of acoustic-gravity waves in inhomogeneous flows of the polar thermosphere. *Journal of Atmospheric and Solar-Terrestrial Physics, 178*, 17–23. https://doi.org/10.1016/j.jastp.2018.05.009

Fedorenko, A. K., Kryuchkov, E. I., Cheremnykh, O. K., & Melnychuk, S. V. (2024). Propagation of acoustic-gravity waves in inhomogeneous wind flows of the polar atmosphere. *Kinematics and Physics of Celestial Bodies*, *40*, 15–23. https://doi.org/10.3103/S0884591324010045

Francis, S. H. (1975). Global propagation of atmospheric gravity waves: A review. *Journal of Atmospheric and Terrestrial Physics*, *37*(6–7), 1011–1030. https://doi.org/10.1016/0021-9169(75)90012-4

Hajkowicz, L. A. (1991). Auroral electrojet effect on the global occurrence pattern of large scale travelling ionospheric disturbances. *Planetary and Space Science*, *39*(8), 1189–1196. https://doi.org/10.1016/0032-0633(91)90170-F

Harvey, V. L., Randall, C. E., Goncharenko, L. P., Becker, E., Forbes, J. M., Carstens, J., Xu, S., France, J. A., Zhang, S.-R., & Bailey, S. M. (2023). CIPS observations of gravity wave activity at the edge of the polar vortices and coupling to the ionosphere. *Journal of Geophysical Research: Atmospheres*, *128*(12), e2023JD038827. https://doi.org/10.1029/2023JD038827

Hays, P. B., Killeen, T. L., & Kennedy, B. C. (1981). The Fabry-Perot interferometer on Dynamics Explorer. *Space Science Instrumentation*, *5*(4), 395–416. https://ntrs.nasa.gov/citations/19820032900

Hines, C. O. (1960). Internal atmospheric gravity waves at ionospheric heights. *Canadian Journal of Physics*, *38*(11), 1441–1481. https://doi.org/10.1139/p60-150

Hocke, K., & Schlegel, K. (1996). A review of atmospheric gravity waves and travelling ionospheric disturbances: 1982–1995. *Annales Geophysicae*, *14*(9), 917–940. https://doi.org/10.1007/s00585-996-0917-6

Innis, J. L., & Conde, M. (2002). Characterization of acoustic-gravity waves in the upper thermosphere using Dynamics Explorer 2 Wind and Temperature Spectrometer (WATS) and Neutral Atmosphere Composition Spectrometer (NACS) data. *Journal of Geophysical Research: Space Physics*, *107*(A12), SIA 1-1–SIA 1–22. https://doi.org/10.1029/2002JA009370

Johnson, F. S., Hanson, W. B., Hodges, R. R., Coley, W. R., Carignan, G. R., & Spencer, N. W. (1995). Gravity waves near 300 km over the polar caps. *Journal of Geophysical Research*, *100*(A12), 23993–24002.

Killeen, T. L., Won, Y.-I., Niciejewski, R. J., & Burns, A. G. (1995). Upper thermosphere winds and temperatures in the geomagnetic polar cap: Solar cycle, geomagnetic activity, and interplanetary magnetic field dependencies. *Journal of Geophysical Research: Space Physics*, *100*(A11), 21327–21342. https://doi.org/10.1029/95JA01208

Lighthill, J. (1978). *Waves in Fluids*. Cambridge University Press.

Liu, H.-L., Lauritzen, P. H., & Vitt, F. (2024). Impacts of Gravity Waves on the Thermospheric Circulation and Composition. *Geophysical Research Letters, 51*(3), e2023GL107453. https://doi.org/10.1029/2023GL107453

Lühr, H., Rentz, S., Ritter, P., Liu, H., & Häusler, K. (2007). Average thermospheric wind patterns over the polar regions, as observed by CHAMP. *Annales Geophysicae*, *25*(5), 1093–1101. https://doi.org/10.5194/angeo-25-1093-2007

Moffat-Griffin, T. (2019). An introduction to atmospheric gravity wave science in the polar regions and first results from ANGWIN. *Journal of Geophysical Research: Atmospheres*, *124*(3), 1198–1199. https://doi.org/10.1029/2019JD030247

Nappo, C. J. (2012). *An Introduction to Atmospheric Gravity Waves* (2nd ed.). Elsevier Science.

Negale, M. R., Taylor, M. J., Nicolls, M. J., Vadas, S. L., Nielsen, K., & Heinselman, C. J. (2018). Seasonal propagation characteristics of MSTIDs observed at high latitudes over Central Alaska using the Poker Flat Incoherent Scatter Radar. *Journal of Geophysical Research: Space Physics, 123*(7), 5717–5737. https://doi.org/10.1029/2017JA024876

Paznukhov, V. V., Sopin, A. A., Galushko, V. G., Kashcheyev, A. S., Koloskov, A. V., Yampolski, Y. M., & Zalizovski, A. V. (2022). Occurrence and characteristics of traveling ionospheric disturbances in the Antarctic Peninsula region. *Journal of Geophysical Research: Space Physics*, *127*(11), e2022JA030895. https://doi.org/10.1029/2022JA030895

Rourke, S., Mulligan, F. J., French, W. J. R., & Murphy, D. J. (2017). A climatological study of short-period gravity waves and ripples at Davis Station, Antarctica (68°S, 78°E), during the (austral winter February–October) period 1999–2013. *Journal of Geophysical Research: Atmospheres, 122*(21), 11,388–11,404. https://doi.org/10.1002/2017JD026998

Spencer, N. W., Wharton, L. E., Niemann, H. B., Hedin, A. E., Carrignan, G. R., & Maurer, J. C. (1981). The Dynamics Explorer wind and temperature spectrometer. *Space Science Instrumentation*, *5*(4), 417–428. https://ntrs.nasa.gov/citations/19820032901

Thayer, J. P., Killeen, T. L., McCormac, F. G., Tschan, C. R., Ponthieu, J. J., & Spencer, N. W. (1987). Thermospheric neutral wind signatures dependent on the east-west component of the interplanetary magnetic field for Northern and Southern Hemispheres as measured by Dynamics Explorer-2. *Annales Geophysicae Series A – Upper Atmosphere and Space Sciences*, *5A*. https://ntrs.nasa.gov/citations/19880035781

Tsugawa, T., Saito, A., & Otsuka, Y. (2004). A statistical study of large-scale traveling ionospheric disturbances using the GPS network in Japan. *Journal of Geophysical Research: Space Physics, 109*(A6), A06302. https://doi.org/10.1029/2003JA010302

Williams, P. J. S., Jones, B., & Jones, G. O. L. (1992). The measured relationship between electric field strength and electron temperature in the auroral E-region. *Journal of Atmospheric and Terrestrial Physics*, *54*(6), 741–748. https://doi.org/10.1016/0021-9169(92)90112-X

Zhang, S.-R., Erickson, P. J., Coster, A. J., Rideout, W., Vierinen, J., Jonah, O., & Goncharenko, L. P. (2019). Subauroral and polar traveling ionospheric disturbances during the 7–9 September 2017 storms. *Space Weather*, *17*(12), 1748–1764. https://doi.org/10.1029/2019SW002325

Received: 26 March 2025
Accepted: 7 May 2025

Вітрове джерело енергії полярних атмосферних гравітаційних хвиль

Алла Федоренко*, Євген Крючков, Анна Войцеховська

Інститут космічних досліджень Національної академії наук України
та Державного космічного агентства України, м. Київ, 03187, Україна

*** Автор для кореспонденції:** fedorenkoak@gmail.com

Реферат. Ми дослідили властивості атмосферних гравітаційних хвиль (АГХ) в областях полярних вітрових систем у термосфері з використанням даних супутникових вимірювань. Встановлено, що АГХ систематично поширюються у напрямку від ночі до дня назустріч вітру. Досліджено залежність амплітуди хвиль від швидкості зустрічного вітру. Показано, що у зустрічній неоднорідній вітровій течії амплітуди хвиль зростають за рахунок енергообміну із середовищем. У результаті, саме такі АГХ великих амплітуд переважають у спостереженнях у полярній термосфері. Тому області вітрової течії можна розглядати як джерело енергії для АГХ. Частоти полярних АГХ були визначені за допомогою супутникових вимірювань. Отримані значення частот для різних полярних орбіт супутника Dynamics Explorer 2 є дуже близькими до частоти Брента-Вяйсяля. Це свідчить про фільтрацію хвильового спектру у неоднорідному вітровому потоці. Отримані результати дозволяють пояснити основні спостережувані зі супутника властивості АГХ у полярній термосфері та порівняти їх із наземними вимірами. При співставленні результатів супутникових та наземних вимірювань характеристик АГХ необхідно враховувати фонові атмосферні течії. Так, частоти АГХ, визначені за супутниковими даними, є близькими до частоти Брента-Вяйсяля. Однак наземний спостерігач реєструватиме такі збурення як дуже низькочастотні. Можна припустити, що частина спостережуваних випадків великомасштабних АГХ є середньомасштабними збуреннями, що поширюються на фоні сильних вітрів. При посиленні геомагнітної активності швидкості полярних вихорів зростають, що супроводжується збільшенням передачі енергії від течії до хвиль у цих областях. Тому АГХ відіграють важливу роль в енергетичному балансі полярної атмосфери, перерозподіляючи енергію збурених вітрових течій у вертикальному напрямку.

Ключові слова: вітрова фільтрація, неоднорідна вітрова течія, полярна термосфера, хвилі в атмосфері